The Resolution of the Gibbs Phenomenon for Fourier Spectral Methods *

Anne Gelb† Sigal Gottlieb‡

December 5, 2006

1 Introduction

Fourier spectral methods have emerged as powerful computational techniques for the simulation of complex smooth physical phenomena. Their exponential convergence rate depends on the smoothness and periodicity of the function in the domain of interest. If the function has a discontinuity at even one point, the convergence rate deteriorates to first order and spurious oscillations develop near the discontinuities. This behavior is called the *Gibbs phenomenon*. The problems that characterize the Gibbs phenomenon are also inherent in Fourier spectral methods applied to partial differential equations with discontinuous solutions. Hence our goal is to present techniques that can significantly reduce the effects of the Gibbs phenomenon to ensure both high order convergence of the Fourier expansion and numerical stability and accuracy of the Fourier spectral method.

In the last few decades, techniques have been developed to mitigate or even completely remove the Gibbs phenomenon in Fourier expansions of discontinuous functions, and there is increasing evidence that some of these methods enable the use of spectral methods for partial differential equations with discontinuous solutions, [1, 10, 11, 12, 13, 14, 36, 40, 41, 42, 43]. This chapter provides an overview of several recent developments in both reducing and overcoming the effects of the Gibbs phenomenon in Fourier expansions, [15, 25, 26, 29, 27, 28, 30, 31, 24, 38]. As a result, it is now possible to use Fourier spectral methods for simulating conservation laws with discontinuous solutions (see references above and [21, 37]). While our focus is on the applications of these techniques to Fourier spectral methods, many of the algorithms presented can also be applied to polynomial spectral methods. The purpose of this chapter is to offer a theoretical introduction, and we strongly encourage the reader to view the above citations for applications and other new developments in this area.

Filtering is a classical tool for mitigating the effect of the Gibbs phenomenon in Fourier expansions. In Section 2 we discuss the use of filters in Fourier expansions of discontinuous functions. However, filtering does not completely remove the Gibbs phenomenon. To completely remove the Gibbs phenomenon, one can re-expand the function in a carefully chosen different basis. In Section 3 we describe the *spectral reprojection* method, which was introduced in [25] and further analyzed in [26, 29, 27, 28, 30, 31]. These two tools have been found to be useful in spectral methods for hyperbolic PDEs; filtering is used to stabilize the method [32, 34], and post-processing to recover

*This work was partially supported by NSF grants CNS 0324957, DMS0608844 and DMS 0510813, and NIH grant EB 025533–01 (AG) and NSF grants DMS0106743 and DMS0608844, and AFOSR grant FA9550-06-1-0255 (SG).

†Department of Mathematics and Statistics, Arizona State University, Tempe, Arizona 85287-1804. Email:ag@math.la.asu.edu

‡Department of Mathematics, University of Massachusetts-Dartmouth, Dartmouth, MA 02747. Email:sgottlieb@umassd.edu

high order of accuracy in smooth regions, [17, 21, 39]. However, to apply the spectral reprojection method in the smooth regions, we require prior identification of the locations of the jump discontinuities. Hence in Section 4 we present an edge detection algorithm based on Fourier spectral data. The method can also be used for uniformly spaced grid point data. Section 5 provides theoretical and numerical arguments for the use of spectral methods for solving partial differential equations with discontinuous solutions. Finally, the techniques of filtering, edge detection, and spectral reprojection are combined to produce numerical results in the Section 6.

2 Filters

One of the manifestations of the Gibbs phenomenon is that the expansion coefficients decay slowly. This is due to the *global* nature of the approximation: the expansion coefficients are obtained by integration or summation over the entire domain, including the points of discontinuity. The idea of filtering is to alter the expansion coefficients so that they decay faster. While this will not impact the non-uniform convergence near the shock, a well chosen filter will improve the convergence rate away from the discontinuity.

A filter of order q is a real and even function $\sigma(\eta) \in C^{q-1}[-\infty, \infty]$ with the following properties:

1.
$$\sigma(\eta) = 0 \quad \text{for} \quad |\eta| > 1.$$

2.
$$\sigma(0) = 1 \quad \text{and} \quad \sigma(1) = 0.$$

3.
$$\sigma^{(m)}(0) = \sigma^{(m)}(1) = 0 \quad \forall m \in [1, \ldots, q-1].$$

A filtered truncated continuous polynomial approximation is

$$f_N^\sigma(x) = \sum_{k=-N}^{N} \sigma(\frac{|k|}{N}) \hat{f}_k \phi_k(x), \tag{2.1}$$

where $\hat{f}_k$ are the expansion coefficients and $\sigma(\frac{|k|}{N})$ is the filter. Note that the filter is a continuous function which only effects the high modes. The fact that the filter is a continuous function is important – cutting off the high modes abruptly (e.g. a step function filter) does not enhance the convergence rate even in smooth regions [25, 44]. Some examples of filters include:

- the second order **Raised Cosine Filter**
$$\sigma(\eta) = \frac{1}{2}\left(1 + \cos\left(\pi\eta\right)\right), \tag{2.2}$$

- the second order **Lanczos filter**
$$\sigma(\eta) = \frac{\sin \pi\eta}{\pi\eta}, \tag{2.3}$$

- and the family of **exponential filters**

$$\sigma(\eta) = \begin{cases} 1 & |\eta| \le \eta_c \\ e^{\left(-\alpha\left(\frac{\eta-\eta_c}{1-\eta_c}\right)^p\right)} & \eta > \eta_c \end{cases}, \tag{2.4}$$

  where α measures the strength of the filter and p is its order.

Note that the exponential filter does not quite conform with the definition of a filter above because $\sigma(1) = e^{-\alpha}$, so α is chosen so that $\sigma(1) \simeq \mathcal{O}(\varepsilon_M)$ where ε_M is the machine accuracy, resulting in the complete removal of the $\pm\frac{N}{2}$ modes. The exponential filter allows the recovery of convergence of any desired order p at any fixed point away from the discontinuity, making it a popular choice when performing simulations of non-linear partial differential equations.

Assume we are given the first $(2N+1)$ Fourier expansion coefficients

$$\hat{f}_k = \frac{1}{2\pi}\int_{-\pi}^{\pi} f(x)e^{-ikx}dx \tag{2.5}$$

of a piecewise analytic function $f(x)$ on $[-\pi, \pi]$, and that the function has a single discontinuity at $x = \xi$. The Fourier partial sum approximation,

$$f_N(x) = \sum_{|k|\le N} \hat{f}_k e^{ikx}, \tag{2.6}$$

yields the Gibbs phenomenon – first order convergence away from the jump discontinuity $x = \xi$ with nonuniform oscillations as the jump discontinuity is approached.

To improve the convergence rate of (2.6), we use the filter $\sigma(\frac{|k|}{N})$, leading to the modified approximation

$$f_N^\sigma(x) = \sum_{|k|\le N} \sigma(\frac{|k|}{N})\hat{f}_k e^{ikx}.$$

Since $\sigma(\eta) = 0$ for $\eta = \frac{|k|}{N} \ge 1$, we have

$$f_N^\sigma(x) = \sum_{|k|<\infty} \sigma(\frac{|k|}{N})\hat{f}_k e^{ikx}.$$

Finally, rearranging terms yields

$$f_N^\sigma(x) = \frac{1}{2\pi}\int_{-1}^{1} S(x-y)f(y). \tag{2.7}$$

where the filter function is given by

$$S(z) = \sum_{|k|<\infty} \sigma(\eta)e^{ikz}. \tag{2.8}$$

Since $f(x)$ is a piecewise $C^p[-\pi, \pi]$ function with a single point of discontinuity at $x = \xi$, the pointwise difference between $f(x)$ and $f_N^\sigma(x)$ at all $x \ne \xi$ is bounded by [25, 44]:

$$|f(x) - f_N^\sigma(x)| \le C_1\frac{1}{N^{p-1}}\frac{1}{d(x)^{p-1}}K(u) + C_2\frac{\sqrt{N}}{N^p}\left(\int_{-\pi}^{\pi}\left|u^{(p)}\right|^2 dx\right)^{1/2}, \tag{2.9}$$

where $d(x) = |x - \xi|$ denotes the distance between a point $x \in [-\pi, \pi]$ and the discontinuity, and

$$K(u) = \sum_{l=0}^{p-1} d(x)^l \left| u^{(l)}(\xi^+) - u^{(l)}(\xi^-) \right| \int_{-\infty}^{\infty} \left| G_l^{(p-l)}(\eta) \right| \, d\eta,$$

with

$$G_l(\eta) = \frac{\sigma(\eta) - 1}{\eta^l}.$$

Hence filtering raises the rate of convergence away from the discontinuity ($d(x) > 0$), as all terms can be bounded by $\mathcal{O}(N^{1-p})$ depending only on the regularity of the piecewise continuous function and the order of the filter. In the case where $f(x)$ is piecewise analytic, one can take the order of the filter $p \propto N$ to yield exponential accuracy at any fixed point away from the discontinuity. The extension to multiple points of discontinuity is straightforward.

3 Spectral Reprojection Methods

3.1 Theoretical Aspects of Spectral Reprojection

While filtering may remove the Gibbs phenomenon away from the discontinuity, the accuracy decreases with proximity to the discontinuity, (2.9). However, if the underlying function is piecewise analytic, the Gibbs phenomenon can be completely removed by re-expanding its Fourier partial sum approximation (2.6) using a different set of basis functions.[1] This idea was first presented in [25] using Gegenbauer polynomials as a reprojection basis for trigonometric polynomials. It was more recently generalized in [31]. In this section we use the interval $[-1, 1]$ and the summation over the nonnegative integers. Fourier series expansions can be easily converted into this notation, which generalizes more easily to orthogonal polynomials.

Assume that $f(x) \in L^2[-1, 1]$ is analytic on some subinterval $[a, b] \subset [-1, 1]$. Let $\{\Psi_k(x)\}$ be an orthonormal family under some inner product product $(\cdot, \cdot)$, and denote the finite continuous expansion in this basis by

$$f_N(x) \; = \; \sum_{k=0}^{N} (f, \Psi_k) \Psi_k(x). \tag{3.1}$$

We assume that

$$|(f, \Psi_k)| \; \leq \; C \tag{3.2}$$

for C independent of k, and that

$$\lim_{N \to \infty} \left(f(x) - f_N(x) \right) \; = \; 0 \tag{3.3}$$

almost everywhere in $x \in [-1, 1]$.

The approximation (3.1) may converge slowly if there is a discontinuity outside of the interval of analyticity $[a, b]$. This is due to the global nature of the expansion: since the coefficients are computed over the entire domain $[-1, 1]$, any discontinuity in that domain will contaminate the expansion – even within the smooth interval $[a, b]$. However, under certain conditions, $f_N(x)$ retains sufficient information to enable the recovery of a high order approximation to $f(x)$ in the interval $[a, b]$. This is accomplished by re-expanding $f_N(x)$ in a different, more appropriate basis.

[1] In fact, the Gibbs phenomenon resulting from any commonly used spectral method (e.g. Chebyshev or Legendre) can be removed by re-expansion into a different, suitable, set of basis functions. The discussion here is limited to the case where the original expansion is the Fourier expansion.

First we define the local variable $\xi \in [-1,1]$ by the transformation

$$\xi = -1 + 2\left(\frac{x-a}{b-a}\right) \tag{3.4}$$

such that if $a \le x \le b$ then $-1 \le \xi \le 1$. Now we re-expand $f_N(x)$ (an expansion in the basis Ψ_k), by an orthonormal family of functions $\{\Phi_k^\lambda\}$ defined in an interval of analyticity $[a,b]$,

$$f_m^\lambda(x) = \sum_{k=0}^{m} < f_N, \Phi_k^\lambda >_\lambda \Phi_k^\lambda(\xi(x)). \tag{3.5}$$

For each fixed λ, the family $\{\Phi_k^\lambda\}$ is orthonormal under some inner product $< \cdot, \cdot >_\lambda$.

This new expansion converges exponentially fast in the interval $[a,b]$ if the family $\{\Phi_k^\lambda\}$ is *Gibbs Complementary* to the family $\{\Psi_k(x)\}$, i.e. if the following three conditions are satisfied:

(a) **Orthonormality**

$$< \Phi_k^\lambda(\xi), \Phi_l^\lambda(\xi) >_\lambda = \delta_{kl} \tag{3.6}$$

for any fixed λ.

(b) **Spectral Convergence**
The expansion of an function $g(\xi)$ which is analytic in $-1 \le \xi \le 1$ (corresponding to $a \le x \le b$), in the basis $\Phi_k^\lambda(\xi)$ converges exponentially fast with $\lambda = \beta m$, i.e.

$$\max_{-1\le\xi\le1} \left| g(\xi) - \sum_{k=0}^{m} < g, \Phi_k^\lambda >_\lambda \Phi_k^\lambda(\xi) \right| \quad \le \quad e^{-q_1\lambda}, \qquad q_1 > 0. \tag{3.7}$$

(c) **The Gibbs Condition**
There exists a number $\beta < 1$ such that if $\lambda = \beta m$ then

$$\left| < \Phi_l^\lambda(\xi), \Psi_k(x(\xi)) >_\lambda \right| \max_{-1\le\xi\le1} \left|\Phi_l^\lambda(\xi)\right| \quad \le \quad \left(\frac{\alpha N}{k}\right)^\lambda$$
$$k > N,\ l \le \lambda,\ \alpha < 1. \tag{3.8}$$

This means that the projection of the high modes of the basis $\{\Psi_k\}$ on the low modes in Φ, that is $\Phi_l^\lambda(\xi)$ with small l, is exponentially small in the interval $-1 \le \xi \le 1$ for λ proportional to N.

Hence a slowly converging series,

$$f_N(x) = \sum_{k=0}^{N} (f, \Psi_k)\Psi_k(x), \tag{3.9}$$

can still yield a rapidly converging approximation to $f(x)$ if one can determine a reprojection basis that satisfies the above three conditions.

As an example, assume that the original expansion is the Fourier partial sum (2.6), with

$$\Psi_k(x) = \frac{1}{\sqrt{2}} e^{ik\pi x}, \tag{3.10}$$

and k running from $-\infty$ to ∞. The orthonormal Gegenbauer polynomials provide an excellent example of a Gibbs complementary family. Thus, any Fourier approximation can be re-expanded in the Gegenbauer basis, and the new approximation known as the Gegenbauer reconstruction method, converges exponentially, [25, 31]. The method is described below.

3.2 Implementation of the Gegenbauer Reconstruction Method

Recall that the Gegenbauer partial sum expansion which converges exponentially for a smooth function $f(x)$ defined in $[-1,1]$ is given by

$$f_m(x) = \sum_{l=0}^{m} \hat{f}_l^{\lambda} C_l^{\lambda}(x), \tag{3.11}$$

where $\hat{f}_l^{\lambda}$ are the Gegenbauer coefficients,

$$\hat{f}_l^{\lambda} = \frac{1}{h_l^{\lambda}} \int_{-1}^{1} (1-x^2)^{\lambda-\frac{1}{2}} C_l^{\lambda}(x) f(x) dx. \tag{3.12}$$

The Gegenbauer polynomials, $C_l^{\lambda}(x)$, are orthogonal under the weight function $(1-x^2)^{\lambda-\frac{1}{2}}$ with

$$\int_{-1}^{1} (1-x^2)^{\lambda-\frac{1}{2}} C_k^{\lambda}(x) C_n^{\lambda}(x) dx = \delta_{k,n} h_k^{\lambda}, \quad h_k^{\lambda} = \pi^{\frac{1}{2}} C_n^{\lambda}(1) \frac{\Gamma(\lambda+\frac{1}{2})}{\Gamma(\lambda)(n+\lambda)}.$$

Clearly, (3.6) and (3.7) are satisfied.

Now let $f(x)$ be a piecewise smooth L_1 function defined in $[-1,1]$ that is analytic in the subinterval $[a,b]$. The interval of smoothness can be effectively determined by the edge detection procedure described in Section 4. By defining a local variable ξ such that $x(\xi) = \epsilon\xi + \delta$, where $\epsilon = \frac{b-a}{2}$ and $\delta = \frac{b+a}{2}$, the Gegenbauer partial sum expansion of $f(x)$ in $[a,b]$ can be written as

$$f_m(x(\xi)) = \sum_{l=0}^{m} \hat{f}_{l,\epsilon}^{\lambda} C_l^{\lambda}(\xi), \quad -1 \le \xi \le 1, \tag{3.13}$$

where the Gegenbauer coefficients $\hat{f}_{l,\epsilon}^{\lambda}$ are defined by

$$\hat{f}_{l,\epsilon}^{\lambda} = \frac{1}{h_l^{\lambda}} \int_{-1}^{1} (1-\xi^2)^{\lambda-\frac{1}{2}} C_l^{\lambda}(\xi) f(\epsilon\xi+\delta) d\xi. \tag{3.14}$$

An exponentially accurate approximation to $\hat{f}_{l,\epsilon}^{\lambda}$ can be constructed as

$$\hat{g}_{l,\epsilon}^{\lambda} = \frac{1}{h_l^{\lambda}} \int_{-1}^{1} (1-\xi^2)^{\lambda-\frac{1}{2}} C_l^{\lambda}(\xi) f_N(\epsilon\xi+\delta) d\xi, \tag{3.15}$$

based on the spectral partial sum expansion (3.9), $f_N(x) = f_N(\epsilon\xi+\delta)$, satisfying (3.8). This approximation replaces $\hat{f}_{l,\epsilon}^{\lambda}$ in the computation of the Gegenbauer partial sum to form the exponentially convergent approximation

$$g_m^{\lambda}(x(\xi)) = \sum_{l=0}^{m} \hat{g}_{l,\epsilon}^{\lambda} C_l^{\lambda}(\xi), \tag{3.16}$$

to $f(x)$ in $[a,b]$ in the maximum norm. Of course the Gegenbauer parameters must be suitably chosen, with $\lambda = \beta m$ and $m = \gamma N$ guaranteeing exponential convergence [31].

Consider the case where (3.9) is given by the Fourier (pseudo-)spectral approximation:

$$f_N(\epsilon\xi+\delta) = \sum_{k=-N}^{N} \hat{f}_k e^{ik\pi(\epsilon\xi+\delta)},$$

where $\hat{f}_k$ is either given by a properly normalized (2.5) or by computing

$$\hat{f}_k = \frac{1}{2N} \sum_{j=0}^{2N-1} f(x_j) e^{-ik\pi x_j}$$

with $x_j = -1 + \frac{j}{N}$, $j = 0, \cdots, 2N-1$. Then the explicit expression [5]

$$\frac{1}{h_l^\lambda} \int_{-1}^{1} (1-\xi^2)^{\lambda - \frac{1}{2}} C_l^\lambda(\xi) e^{ik\pi(\epsilon\xi+\delta)} d\xi = \Gamma(\lambda)(\frac{2}{\pi k})^\lambda i^l (l+\lambda) J_{l+\lambda}(\pi k),$$

is exploited to obtain

$$\hat{g}_{l,\epsilon}^\lambda = \delta_{0,l}\hat{f}_0 + \Gamma(\lambda) i^l (l+\lambda) \sum_{0<|k|\le N} J_{l+\lambda}(\pi k\epsilon)(\frac{2}{\pi k\epsilon})^\lambda \hat{f}_k e^{ik\pi\delta}. \tag{3.17}$$

This allows use of the efficient FFT algorithm and avoids a more expensive quadrature formulation. To show the efficacy of the Gegenbauer reconstruction method, we consider the following example:

Example 3.1 $f(x) = \cos(1.4\pi(x-1)), \quad -1 \le x \le 1.$

Figure 3.2 exhibits the results for the Gegenbauer reconstruction method using the parameters $\lambda = m = \frac{1}{4}N$ and $\lambda = m = \frac{2}{5}N$. The results concur with those in [25]. We note that it is possible to optimize the parameters λ and m according to the error bounds and underlying smoothness of $f(x)$ [16, 22].

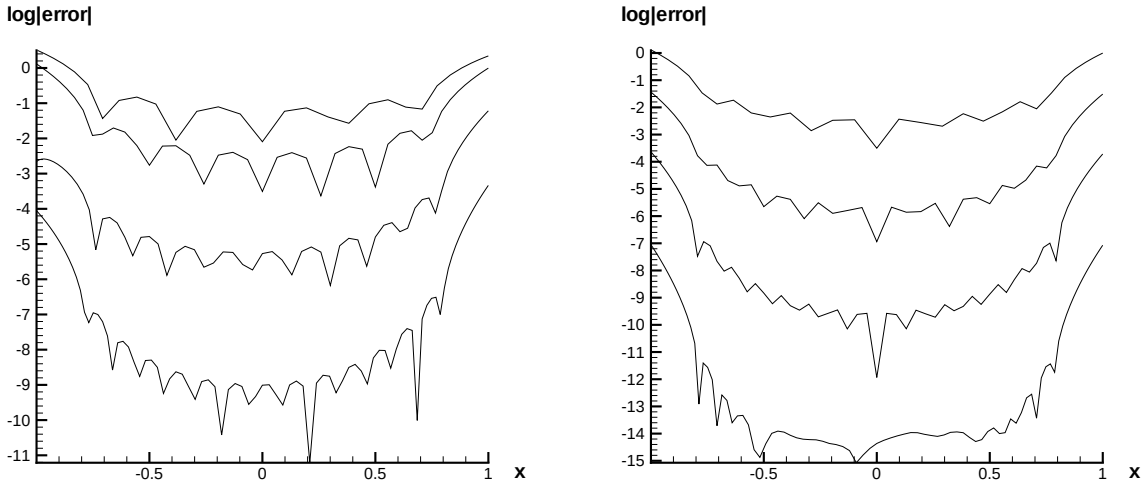

Figure 1: The errors in logarithmic scale for the Gegenbauer reconstruction method applied to example 3.1 with $N = 16, 24, 36, 52$ when (a) $\lambda = m = \frac{1}{4}N$ and (b) $\lambda = m = \frac{2}{5}N$.

The numerical results for Example 3.1 show that the Gegenbauer reconstruction method is effective in eliminating the Gibbs phenomenon for a certain class of (analytic) functions. This theory can be used to find Gibbs complementary functions for any set of functions, and Chebyshev and Legendre polynomials both have Gegenbauer polynomials as Gibbs complementary bases [34]. There have been many results since then that describe some of the difficulties in using the Gegenbauer reconstruction

method, [7, 22, 23, 38]. Specifically, round off error is a major drawback in computation, as is the tendency of the Gegenbauer partial sum expansion to behave like a power series, which corresponds to a Runge phenomenon type behavior [7, 22]. As a result, it is useful to consider other types of reprojection bases. For instance, the Freud polynomials considered in [23] were shown to yield spectral accuracy without negative effects caused by round off error or Runge phenomenon when the original projection (3.9) is a Fourier partial sum expansion. It is likely that Freud polynomials can also be used when (3.9) is a Chebyshev or Legendre approximation. Research will continue in this area of finding appropriate reprojection bases, and it is possible that the optimal bases may not be polynomials at all.

4 Discontinuity Detection

In this section we describe an edge detection procedure, originally developed in [18], which recovers the location and amplitudes of jump discontinuities of a piecewise smooth function $f(x)$ from either continuous Fourier spectral coefficients or discrete ones based on equally spaced grid values in physical space. Edge detection is necessary to determine the intervals of smoothness in which the piecewise smooth function can be reconstructed by the spectral reprojection method.

The detectors presented here effectively resolve the corresponding jump function, $[f](x)$, so that edges are detected by separation. Specifically, the detectors "concentrate" near the $\mathcal{O}(\infty)$ scale of jump discontinuities which are effectively separated from the smooth regions where $[f](x) \sim 0$. This procedure, coined "the concentration method", offers a large family of edge detectors, each detector associated with its own particular concentration factor. The prescribed procedure is computationally efficient and robust. There are, whoever, two major drawbacks. First, in order to "pinpoint" the edges, which is necessary to define each region of smoothness, one has to introduce an outside threshold parameter to quantify the "large" jumps, i.e., those with $[f](x) \gg \mathcal{O}(\Delta x)$, implying that the edge detection method is inherently problem dependent, [19]. Second, oscillations form in the neighborhood of the jump discontinuities. The particular behavior of these oscillations depends on the specific concentration factors used. Therefore it can be difficult to distinguish what constitutes a true jump discontinuity as opposed to an oscillating artifact, particularly when several jump discontinuities are located in the same neighborhood, i.e. when there is limited resolution. An adaptive, parameter-free edge detection procedure based on the nonlinear limiting of low- and high-order concentration factors was introduced in [20]. In this work, the authors used the so-called minmod limiter to retain the high-order in smooth regions while "limiting" the high-order spurious oscillations in the neighborhoods of the jumps by the less oscillatory low-order detectors. Below we review the basic construction of the concentration edge detection method and use of the minmod limiter when the Fourier coefficients of a piecewise smooth function are known. The extension to other spectral bases and discrete data, as well as proofs regarding the convergence of the method to the jump discontinuities, can be found in [18, 19, 20].

4.1 Discontinuity Detection by Concentration Kernels

Assume that $f(x)$, $x \in [-\pi, \pi)$, is a piecewise smooth function with jump discontinuities that have well defined one-sided limits, $f(x\pm) = \lim_{x \to x\pm} f(x)$, and let $[f](x) := f(x+) - f(x-)$ denote the

local jump function. We define piecewise smoothness as[2]

$$F_x(t) := \frac{f(x+t) - f(x-t) - [f](x)}{t} \in BV[0,\delta], \qquad \forall x. \tag{4.1}$$

In practice $f(x)$ has a finite number of jump discontinuities, and (4.1) requires the differential of $f(x)$ on each side of the discontinuity to have bounded variation. For example, if $f'(x\pm)$ are well defined for finitely many jumps, then (4.1) holds.

The edges in piecewise smooth $f(x)$ are detected using smooth *concentration kernels*, $K(t) = K_\epsilon(t)$, which are characterized by

$$K_\epsilon * f(x) \longrightarrow [f](x) \qquad \text{as } \epsilon \to 0, \tag{4.2}$$

where ϵ is a small parameter inversely proportional to the number of Fourier coefficients. Thus the support of $K_\epsilon * f(x)$ tends to "concentrate" near the edges of $f(x)$ and both the location of the jump discontinuities as well as their amplitudes can be recovered.

The concentration property of K_ϵ is guaranteed by the following properties:

1. K_ϵ is *odd*:
$$K_\epsilon(-t) = -K_\epsilon(t). \tag{4.3}$$

2. K_ϵ is normalized so that
$$\int_{t\geq 0} K_\epsilon(t)dt = -1 + \mathcal{O}(\epsilon). \tag{4.4}$$

3. The main *admissibility requirement* is satisfied:
$$\left| \int_t tK_\epsilon(t)\phi(t)dt \right| \leq Const \cdot \epsilon ||\phi||_{BV}. \tag{4.5}$$

Remark: If $K_\epsilon(t)$ concentrates near the origin, for example, so that its first moment does not exceed

$$\int_t |tK_\epsilon(t)|dt \leq Const \cdot \epsilon, \tag{4.6}$$

then it is clearly admissible in the sense that (4.5) holds. However, the admissibility condition also allows for more general oscillatory kernels, $K_\epsilon(t)$, where (4.6) might not hold, yet (4.5) is satisfied due to the cancellation effect of the oscillations. This will prove useful later when the minmod limiter is applied, since oscillations of different signs will be eliminated from the approximation. The main result from [19] states that

Theorem 4.1 *Consider an odd kernel $K_\epsilon(t)$, (4.3), normalized so that (4.4) holds, and satisfying the admissibility requirement (4.5). Then the kernel $K_\epsilon(t)$ satisfies the concentration property (4.2) for all piecewise smooth f's, and the following error estimate holds*

$$|K_\epsilon * f(x) - [f](x)| \leq Const \cdot \epsilon. \tag{4.7}$$

[2]Here and below we use $BV[a,b]$ to denote the space of functions with bounded variation, endowed with the usual semi-norm $\|\phi\|_{BV[a,b]} := \int_a^b |\phi'|dx$

Proof. Since $K_\epsilon(t)$ is odd, we have

$$\begin{aligned} K_\epsilon * f(x) &= -\int_{t\geq 0} K_\epsilon(t)(f(x+t)-f(x-t))dt \\ &= -\int_{t\geq 0} tK_\epsilon(t)\frac{f(x+t)-f(x-t)-[f](x)}{t}dt - [f](x)\int_{t\geq 0} K_\epsilon(t)dt. \end{aligned}$$

Applying (4.4) yields

$$K_\epsilon * f(x) - [f](x) = -\int_{t\geq 0} tK_\epsilon(t)F_x(t)dt + \mathcal{O}(\epsilon). \tag{4.8}$$

By the assumption in (4.1), $F_x(t)$ is BV and it is therefore bounded. Consequently, in the particular case that the moment bound (4.6) holds, the first term on the right of (4.8) is of order $\mathcal{O}(\epsilon)$, yielding

$$|K_\epsilon * f(x) - [f](x)| \leq Const \cdot \int |tK_\epsilon(t)|dt + \mathcal{O}(\epsilon) = \mathcal{O}(\epsilon).$$

In the general case, $F_x(t)$ has bounded variation, and the admissibility requirement (4.5) implies that the first term on the right of (4.8) is of order $\mathcal{O}(\epsilon)$, and we conclude

$$|K_\epsilon * f(x) - [f](x)| \leq Const||F_x(t)||_{BV} \cdot \epsilon + \mathcal{O}(\epsilon) = \mathcal{O}(\epsilon).$$

4.2 Examples of Concentration Kernels

4.2.1 Compactly supported kernels

Our first example consists of concentration kernels which "concentrate" near the origin, so that (4.6) holds. We consider a standard mollifier, $\phi_\epsilon(t) := \frac{1}{\epsilon}\phi(\frac{t}{\epsilon})$, based on an even, compactly supported bump function, $\phi \in C_0^1(-1,1)$ with $\phi(0) = 1$. We then set

$$K_\epsilon(t) = \frac{1}{\epsilon}\phi'(\frac{t}{\epsilon}) \equiv \phi'_\epsilon(t). \tag{4.9}$$

Clearly, K_ϵ is an odd kernel satisfying the required normalization (4.4)

$$\int_{t\geq 0} K_\epsilon(t)dt = \frac{1}{\epsilon}\int_{t\geq 0}\phi'(\frac{t}{\epsilon})dt = -\phi(0) = -1.$$

In addition, its first moment is of order

$$\int_{t\geq 0} |tK_\epsilon(t)|dt = \epsilon\int_{0\leq s\leq 1} |s|\dot{|}\phi'(s)|ds = \mathcal{O}(\epsilon),$$

and hence (4.6) holds. Theorem 4.1 then implies

Corollary 4.1 *Consider the odd kernel $K_\epsilon(t) = \phi'_\epsilon(t)$, based on even $\phi \in C_0^1(-1,1)$ with $\phi(0) = 1$. Then $K_\epsilon(t)$ satisfies the concentration property (4.2), and the following error estimate holds*

$$\phi'_\epsilon * f(x) = [f](x) + \mathcal{O}(\epsilon). \tag{4.10}$$

4.2.2 The conjugate Dirichlet kernel

The conjugate Dirichlet kernel,

$$K_N(t) = -\frac{1}{\log N}\tilde{D}_N(t), \qquad \tilde{D}_N(t) := \sum_{k=1}^{N} \sin kt,$$

is an example of an oscillatory concentration kernel. Clearly, $K_N(t)$ is an odd kernel. Moreover, the normalization (4.4) holds with $\epsilon \sim \frac{1}{\log N}$,

$$\int_{t=0}^{\pi} K_N(t)dt = -\frac{2}{\log N} \sum_{\text{odd } k's} \frac{1}{k} = -1 + \mathcal{O}(\epsilon), \quad \epsilon \sim \frac{1}{\log N}.$$

Finally, summing

$$\tilde{D}_N(t) = \sum_{k=1}^{N} \sin kt = \frac{\cos\frac{t}{2} - \cos(N+\frac{1}{2})t}{2\sin\frac{t}{2}},$$

we find that the first moment of $K_N = -\tilde{D}_N(t)/\log N$ does not exceed

$$\int_{t=0}^{\pi} |tK_N(t)|dt \le Const \cdot \epsilon, \quad \epsilon = \frac{1}{\log N},$$

so that the requirement (4.6) is fulfilled.

Theorem (4.1) then yields the classical result regarding the concentration of conjugate partial sums, [4, §42],[45, §II Theorem 8.13],

$$-\frac{1}{\log N}\tilde{D}_N * f(x) = [f](x) + \mathcal{O}(\frac{1}{\log N}). \tag{4.11}$$

We note in passing that in the case of Dirichlet conjugate kernel, $K_N(t)$ does not concentrate near the origin, but instead (4.6) is fulfilled thanks to its uniformly small amplitude of order $\mathcal{O}(1/\log N)$. The error, however, is only of logarithmic order, [18].

4.2.3 Oscillatory kernels (general concentration factors)

To accelerate the unacceptable logarithmically slow rate of Dirichlet conjugate kernel in (4.11), we consider general form of odd concentration kernels

$$K_N^{\tau}(t) := -\sum_{k=1}^{N} \tau(\frac{k}{N}) \sin kt, \tag{4.12}$$

based on *concentration factors*, $\tau(\frac{k}{N})$ which are yet to be determined. Clearly $K_N^{\tau}(t)$ is odd. Next, for the normalization (4.4) we note that

$$\int_{t=0}^{\pi} K_N^{\tau}(t)dt = -2 \sum_{k \text{ odd}} \frac{\tau(\frac{k}{N})}{k} \sim -\int_0^1 \frac{\tau(x)}{x}dx.$$

In fact, the above Riemann's sum amounts to the midpoint quadrature, so that for $\frac{\tau(\xi)}{\xi} \in C^2[0,1]$, one has

$$\int_{t=0}^{\pi} K_N^{\tau}(t)dt = -2 \sum_{k \text{ odd}} \frac{\tau(\frac{k}{N})}{k} = -\int_0^1 \frac{\tau(\xi)}{\xi}d\xi + \mathcal{O}(\frac{1}{N^2}), \tag{4.13}$$

and thus (4.4) holds for normalized concentration factors $\tau(\xi)$,

$$\int_0^1 \frac{\tau(\xi)}{\xi} d\xi = 1. \tag{4.14}$$

Finally, we address the admissibility requirement (4.5) (and in particular (4.6)). Let $\xi_k = \frac{k}{N}$. We use the identity

$$\begin{aligned} 2\sin(t/2)K_N^\tau(t) &\equiv \sum_{k=1}^{N-2}(\tau(\xi_k) - 2\tau(\xi_{k+1}) + \tau(\xi_{k+2}))\frac{\sin(k+1)t}{2\sin(t/2)} \\ &- (\tau(1) - \tau(\xi_{N-1}))\frac{\sin Nt}{2\sin(t/2)} + (\tau(\xi_2) - \tau(\xi_1))\frac{\sin t}{2\sin(t/2)} \\ &+ \tau(\xi_1)\cos\frac{t}{2} - \tau(1)\cos(N+\frac{1}{2})t = \\ &=: I_1(t) + I_2(t) + I_3(t) + I_4(t) - I_5(t). \end{aligned} \tag{4.15}$$

This leads to the corresponding decomposition of $K_N^\tau(t)$

$$K_N^\tau(t) = R_N^\tau(t) - \frac{\tau(1)}{2}\frac{\cos(N+\frac{1}{2})t}{\sin\frac{t}{2}}.$$

Here, $R_N^\tau(t)$ consists of the first four terms on the right hand side of (4.15), $\sum_{j=1}^4 I_j(t)/2\sin(t/2)$, and it is easily verified that each one of these terms has a small first moment satisfying (4.6) (and consequently, (4.5) holds), i.e.

$$\int_{t=0}^{\pi} |tR_N^\tau(t)|dt \le Const \cdot ||\tau||_{C^2[0,1]}\frac{\log N}{N}. \tag{4.16}$$

For example, using the standard bound $|\sin(kt)/2\sin(t/2)| \le \min\{k, 1/t\}$, the contribution corresponding to the first term, $I_1(t)$, does not exceed

$$\int_{t=0}^{\pi}\left|t\frac{I_1(t)}{2\sin(t/2)}\right|dt \le \frac{\max|\tau''|}{N^2}\sum_{k=1}^{N-2}\left[\int_{t=0}^{1/N} + \int_{t=1/N}^{\pi}\right]\left|\frac{\sin(kt)}{2\sin(t/2)}\right|dt = \mathcal{O}(\frac{\log N}{N}).$$

Similar estimates hold for the remaining contributions of I_2, I_3 and I_4. In particular, since $\tau(\xi)/\xi$ is bounded, $|\tau(1/N)| \le \mathcal{O}(1/N)$, and hence $\int |tI_4(t)/2\sin(t/2)|dt = \mathcal{O}(1/N)$.

Finally, the admissibility of the fifth term on the right of (4.15) is due to standard cancellation which guarantees that (4.5) holds,

$$\left|\frac{\tau(1)}{2}\int_{t=0}^{\pi} t\frac{\cos(N+\frac{1}{2})t}{\sin\frac{t}{2}}\phi(t)dt\right| \le Const \cdot \frac{\tau(1)}{N}||\phi||_{BV}. \tag{4.17}$$

It is in this context of spectral concentration kernels that admissibility requires the more intricate property of cancellation of oscillations. Summarizing (4.13), (4.16) and (4.17), we obtain as a corollary of the main result regarding spectral edge detection using concentration kernels, $K_N^\tau(t)$. In particular, since $K_N^\tau(t)$ are $N-$degree trigonometric polynomials, one detects the edges of the piecewise smooth function $f(x)$ directly from its spectral projection $S_N(f) := \sum_{k=-N}^N \hat{f}_k e^{ikx}$,

$$K_N^\tau * f \equiv K_N^\tau * S_N(f) = i\pi\sum_{k=-N}^{N} sgn(k)\tau(\frac{|k|}{N})\hat{f}_k e^{ikx}.$$

Corollary 4.2 *Consider the odd concentration kernel (4.12)*

$$K_N^\tau(t) = -\sum_{k=1}^{N} \tau(\frac{k}{N}) \sin kt, \qquad \frac{\tau(\xi)}{\xi} \in C^2[0,1].$$

Assume that $\tau(\cdot)$ is normalized so that (4.14) holds

$$\int_0^1 \frac{\tau(\xi)}{\xi} d\xi = 1.$$

Then $K_N^\tau(t)$ admits the concentration property (4.2), and the following estimate holds

$$|K_N^\tau * S_N(f) - [f](x)| = Const \cdot \frac{\log N}{N}. \tag{4.18}$$

We note that the error estimate in (4.18) is valid throughout the interval, including at the location of the jump discontinuities.

We write the concentration method as

$$\tilde{S}_N^\tau[f](x) := i\pi \sum_{k=-N}^{N} sgn(k) \tau(\frac{|k|}{N}) \hat{f}_k e^{ikx}, \tag{4.19}$$

noting the proof in [4] for $\tau(\xi) = 1$:

$$\tilde{S}_N[f](x) := i\pi \sum_{k=-N}^{N} sgn(k) (\frac{|k|}{N}) \hat{f}_k e^{ikx} \to \log N[f](x).$$

Some examples of (oscillatory) concentration factors include:

1. Trigonometric factors of the form

$$\tau(\xi) = \tau_\alpha(\xi) := \sin \alpha\xi / Si(\alpha) \tag{4.20}$$

with the proper normalization $Si(\alpha) := \int_0^\alpha (\sin \eta/\eta) d\eta$.

2. Polynomial factors of the form

$$\tau(\xi) = \tau^p(\xi) := p\xi^p. \tag{4.21}$$

For p odd, $K_N^{\tau^p} * f = (-1)^{[p/2]} p N^{-p} S_N^{(p)}(f)$ and for p even, $K_N^{\tau^p} * f = (-1)^{p/2} p N^{-p} H * S_N^{(p)}(f)$ where $H(x) = i \sum sgn(k) e^{ikx}$. Corollary 4.2 yields

$$\left| \frac{i\pi}{N^p} \sum_{k=-N}^{N} sgn(k)|k|^p \hat{f}_k e^{ikx} - [f](x) \right| \le Const \cdot \frac{\log N}{N}.$$

The last error estimate is (essentially) first order. It is sharp. The polynomial factor τ^p with higher p lead to faster convergence rate at selected interior points, bounded away from the singularities of f.

3. Exponential factors of the form:

$$\tau^{exp}(\xi) = Const \cdot \xi e^{\frac{1}{\gamma\xi(\xi-1)}}, \qquad Const = \int exp\Big(\frac{-1}{\gamma\eta(\eta-1)}\Big) d\eta \tag{4.22}$$

normalized so that $\int_{\xi=0}^1 \tau^{exp}(\xi)/\xi d\xi = 1$.

Polynomial concentration factors (of odd degree) correspond to differentiation in physical space; trigonometric factors correspond to divided differences in the physical space [3]. Our main result stated in Corollary 4.2 provides us with the framework of general concentration kernels which are not necessarily limited to a realization in the physical space. In particular, the exponential concentration factors (4.22) vanish at $\xi = 0, 1$ to any prescribed order,

$$\frac{d^j}{d\xi^j}\tau(\xi)\Big|_{\xi=0} = \frac{d^j}{d\xi^j}\tau(\xi)\Big|_{\xi=1} = 0, \qquad j = 0, 1, 2, \ldots, p-1. \tag{4.23}$$

The higher p is, the more localized the corresponding concentration kernel, $K_N^\tau(\cdot)$ becomes, [19]. This is because $K_N^\tau(t_\ell)/N$ coincide with the ℓ-discrete Fourier coefficient of $\tau(\cdot)$, and since $\tau(\xi)$ and its first p-derivatives vanish with at both ends, $\xi = 0, 1$, there is a rapid decay of its (discrete) Fourier coefficients, $|\hat{\tau}_\ell| \leq Const.\ell^{-p}$ so that

$$|K_N^\tau(t_\ell)| \leq Const.\|\tau\|_{C^{p+1}[0,1]}\frac{1}{(Nt_\ell)^p}.$$

Thus, for t away from the origin, $K_N^\tau(t)$ is rapidly decaying for large enough N's.

To demonstrate the detection of edges by the concentration factors outlined above, consider the following example of a discontinuous function defined on $[-\pi, \pi]$:

Example 4.1

$$f(x) = \begin{cases} \frac{1}{2}\cos 3x + \frac{1}{2} & -\pi \leq x < -\frac{\pi}{2} \\ \frac{4}{1+2x^2} - 2 & -\frac{\pi}{2} \leq x < \frac{\pi}{2} \\ \sin x \cos\frac{7x}{2} & \frac{\pi}{2} \leq x < \pi. \end{cases} \tag{4.24}$$

Assume we are given the Fourier coefficients of $f(x)$ and we wish to recover its corresponding jump function:

$$[f](x) = \begin{cases} \frac{6-5\pi^2}{4+2\pi^2} \approx -1.83 & x = -\frac{\pi}{2} \\ \frac{1}{\sqrt{2}} - \frac{4-2\pi^2}{2+\pi^2} \approx 2.03 & x = \frac{\pi}{2} \\ 0 & \text{elsewhere.} \end{cases} \tag{4.25}$$

Figure 2 demonstrates the use of the various concentration factors in the concentration method for detecting edges. Note the improved localization of the exponential concentration factor (4.22).

Figure 2 shows that the concentration method (4.19) does indeed "concentrate" at the discontinuities of fnctions. However, it is also apparent that there are some problems. Specifically, oscillations that occur in the neighborhood of a jump discontinuity can be misidentified as true edges. On the other hand, using some of the lower-order concentration factors increase the risk of identifying a steep gradient as an edge, especially when few Fourier coefficients are originally known. This is further complicated when jump discontinuities are located near to each other, since the oscillations occurring in the neighborhoods of each discontinuity interfere with the true jump discontinuities. There are distinctions between the different concentration factors that can be exploited in determining the true jumps from the artificial oscillations or the steep unresolved gradients, however. Although the first order polynomial edge detection (4.21) has slow convergence away from the discontinuities, there are few oscillations in the neighborhoods of the discontinuities. On the other hand, the exponential concentration factor (4.22) suffers from severe oscillations within the neighborhoods, but produces rapid convergence to zero away from the neighborhoods of discontinuities, This loss of monotonicity with the increasing order is, of course, the canonical situation in many numerical algorithms. In [20], an adaptive edge detection procedure was introduced that realizes the strengths of various concentration factors used in the edge detection method. That is, away from the jumps, the exponentially

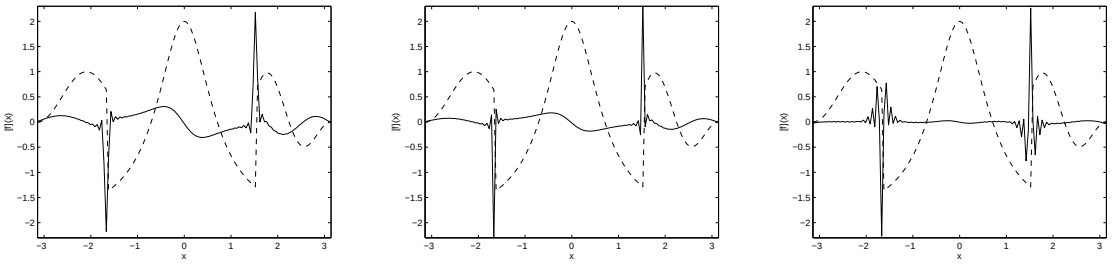

(a) **(b)** **(c)**

Figure 2: The concentration method, (4.19) with $N = 64$, applied to Example 4.1 using (a) Trigonometric factor with $\alpha = \pi$, (b) Polynomial factor with $p = 1$, and (c) exponential factor with $Const = 3$ and $\gamma = 6$. In all three figures the underlying function is dashed and the jump function approximation is solid.

small factors dominates the approximation by taking the *smallest* (in absolute) value between the low-order and high-order detectors. As the jump discontinuity is approached, the spurious oscillations produced by the high-order method should be rejected by the low-order detectors: hence, when two values disagree in sign, indicating spurious oscillations, the detectors should be set to zero. We end up with the so-called *minmod* limiter which plays a central role in non-oscillatory reconstruction of high-resolution methods for nonlinear conservation laws, (e.g., [33, 43] and the references therein), and has been used in the context of edge detection in [6]. The *minmod* limiter is:

$$\widetilde{S}_N^{minmod}[f](x) = minmod(\tilde{S}_N^{\tau^{exp}}[f](x), \tilde{S}_N^{\tau^p}[f](x), \tilde{S}_N^{\tau_\alpha}[f](x)), \tag{4.26}$$

where the k-tuple *minmod* operation takes the form

$$minmod\{a_1, a_2, \ldots, a_k\} := \begin{cases} s \cdot min(|a_1|, |a_2|, \ldots, |a_k|) & \text{if } sgn(a_1) = \ldots = sgn(a_k) := s \\ \\ 0 & \text{otherwise.} \end{cases} \tag{4.27}$$

Our numerical results indicate using the three different concentration factors, (4.20), (4.21), and (4.22), is enough to remove most of the unwanted oscillations from the jump function approximation. Typically $p = 1$, $\alpha = \pi$ and τ^{exp} with $Const = 3$ and $\gamma = 6$ yield approximations converging to the jump function with very few oscillations. Figure 3 displays these results.

What is remarkable about the *minmod* approximation is that no outside scaling parameter is introduced to determine what qualifies as an edge. Hence small scale features can be recognized and the edges can be located at very close distances. This has been shown to be extremely important in brain MRI applications [2], where various tissue regions must be identified with a small number of Fourier coefficients. Of course, some outside thresholding must be introduced when noise in the problem is comparable to the jump magnitudes, [20]. Finally, we note that the concentration method has been developed for other spectral expansions in [19], and has been used for post-processing Legendre approximations of Burgers and Euler's equations. In the case of Euler's equation, they were also used to find edges in the derivatives [21].

4.3 Recent Advances in the Concentration Method

Using the *minmod* limiter (4.26) has dramatically improved the results of the concentration method, (4.19). However, it is clear from Figure 3 that some thresholding is still needed to completely remove

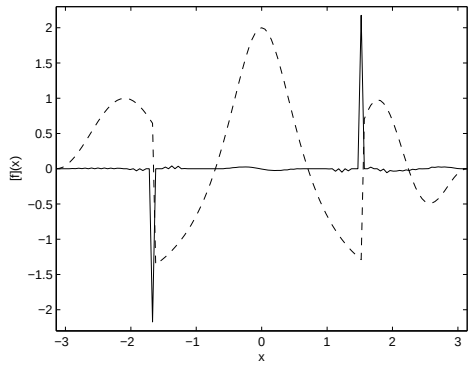

Figure 3: The minmod limiter, (4.26), applied to Example 4.1 using the concentration factors (4.20), (4.21) and (4.22). The underlying function is dashed and the jump function approximation is solid.

the remaining oscillations. One way to improve the results is to filter the oscillations produced by the concentration method. Care must be exercised, however, since too much filtering will potentially lose jump locations. In [9], it was shown that applying a Lanczos filter, (2.3), of different orders directly to the concentration method resulted in a new family of admissible concentration factors:

$$\tau_f(\eta) = \frac{1}{\gamma_n}\tau(\eta)(\frac{\sin \pi\eta}{\pi\eta})^n, \tag{4.28}$$

for $n = 1, 2, \cdots$. Here γ_n is a normalization constant defined by

$$\gamma_n := \int_\epsilon^1 \frac{\tau(\eta)}{\eta}\tau_L^n(\eta)d\eta.$$

Other filters, (2.2) and (2.4), could also be applied yielding similar results. Filtered concentration factors are preferred when noise is present in the underlying function, [9].

To further reduce the method induced oscillations, another technique was introduced in [9] that takes advantage of the fact that each concentration factor, either filtered or unfiltered, generates its own signature profile, or waveform, defined for $x \in [-\pi, \pi)$ as:

$$W_N^\tau(x) := \sum_{k=1}^N \tau(\frac{k}{N})\frac{\cos kx}{k}. \tag{4.29}$$

An alternative derivation [9, 18] of the convergence estimate of the concentration method (4.19) leads directly to the waveform (4.29), and is reproduced here.

For simplicity, we consider a single jump discontinuity and note that the process is easily extended to include any finite number of jumps. We begin by integrating the Fourier coefficients (2.5) by parts to obtain

$$\hat{f}_k = -\frac{i}{2\pi k}[f](\xi)e^{-ik\xi} - \frac{i}{2\pi k}\int_{-\pi}^{\pi} f'(\tau)e^{-ik\tau}\ d\tau. \tag{4.30}$$

Substituting (4.30) into the concentration method, (4.19), yields

$$\begin{aligned}\tilde{S}_N^\tau[f](x) &= i\pi\sum_{k=-N}^N sgn(k)\tau(\frac{|k|}{N})\Big[\frac{-i}{2\pi k}[f](\xi)e^{-ik\xi} - \frac{i}{2\pi k}\int_{-\pi}^{\pi} f'(\tau)e^{-ik\tau}d\tau\Big]e^{ikx} \\ &= \frac{1}{2}[f](\xi)\sum_{k=-N}^N sgn(k)\tau(\frac{|k|}{N})\frac{e^{ik(x-\xi)}}{k} + R(x),\end{aligned} \tag{4.31}$$

where the residual $R(x)$ is defined as

$$\begin{aligned} R(x) &:= \frac{1}{2}\sum_{k=-N}^{N}\frac{1}{k}sgn(k)\tau(\frac{|k|}{N})\int_{-\pi}^{\pi}f'(\tau)e^{-ik(\tau-x)}d\tau \\ &= \sum_{k=1}^{N}\frac{1}{k}\tau(\frac{k}{N})\int_{-\pi}^{\pi}f'(\tau)\cos k(\tau-x)d\tau. \end{aligned} \tag{4.32}$$

Since $\tau(\frac{k}{N})$ is bounded and the integral is $\mathcal{O}(\frac{1}{k})$, we have $R(x)\to 0$ as $N\to\infty$ with $\mathcal{O}(\frac{1}{N})$.[3] Therefore, (4.31) yields

$$\begin{aligned} \tilde{S}_N^{\tau}[f](x) &= \frac{[f](\xi)}{2}\sum_{k=-N}^{N}sgn(k)\tau(\frac{|k|}{N})\frac{e^{ik(x-\xi)}}{k}+\mathcal{O}(\frac{1}{N}) \\ &= [f](\xi)\sum_{k=1}^{N}\tau(\frac{k}{N})\frac{\cos k(x-\xi)}{k}+\mathcal{O}(\frac{1}{N}), \end{aligned} \tag{4.33}$$

leading to the definition of the matching waveform in (4.29). Clearly,

$$W_N^{\tau}(x-\xi)=\delta_{\xi}(x)+\mathcal{O}(\frac{1}{N}), \tag{4.34}$$

where $\delta_{\xi}(x)$ is the Kronecker delta function.

The distinct form of $\tilde{S}_N^{\tau}[f](x)$ is therefore given by $W_N^{\tau}(x-\xi)$ which represents the shape which the concentration method should produce when it locates a simple unit step jump discontinuity at $x=\xi$. This exact shape may not be generated due to the structure of the underlying function, the relative positions of adjacent jumps, or noise. However, convolving the traditional concentration method, (4.19), with its signature profile, (4.29), generates areas of best match which are the likely candidates for the simple jump discontinuity locations. Note that $W_N^{\tau}(x-\xi)$ depends on the concentration factor employed, the location of the jump discontinuity, and N, but to within a proportionality constant, it does not depend on the underlying function.

This observation led to the definition of a new family of concentration factors coined the "matching waveform concentration factors" in [9]. In fact, the edge detection method was derived as the convolution

$$\tilde{M}_N^{\tau}[f](x):=\gamma_M^{\tau}(N)(\tilde{S}_N^{\tau}[f]*W_N^{\tau})(x). \tag{4.35}$$

Here, $\gamma_M^{\tau}(N)$ is used to normalize $\tilde{M}_N^{\tau}[f](x)$ and ensures that that the correct signed magnitude of the jump function is recovered. This is accomplished by requiring $\tilde{M}_N^{\tau}[f](x)|_{x=\xi}=1$ in the case where $\tilde{S}_N^{\tau}[f](x)=W_N^{\tau}(x)$, yielding

$$\frac{1}{\gamma_M^{\tau}(N)}:=\frac{1}{\pi}(W_N^{\tau}*W_N^{\tau})(x)\Big|_{x=\xi}=\frac{1}{\pi}\int_{-\pi}^{\pi}(W_N^{\tau}(\tau))^2d\tau. \tag{4.36}$$

It was further shown in [9] that (4.35) can be rewritten in the form of (4.19) as

$$\tilde{M}_N^{\tau}[f](x)=i\pi\sum_{k=-N}^{N}sgn(k)\tau_M(\frac{|k|}{N})\hat{f}_k\exp(ikx), \tag{4.37}$$

[3] This error estimate is a worst case scenario. Other choices of concentration factors yield higher order convergence away from the jump discontinuities, [18, 19].

where we have defined

$$\tau_M(\frac{|k|}{N}) := \gamma_M^\tau(N)\tau(\frac{|k|}{N})\int_{-\pi}^{\pi} W_N^\tau(\tau)\exp(-ik\tau)d\tau. \tag{4.38}$$

Figure 4 demonstrates the reduced numerical oscillations in the concentration method when the new concentration factors are applied.

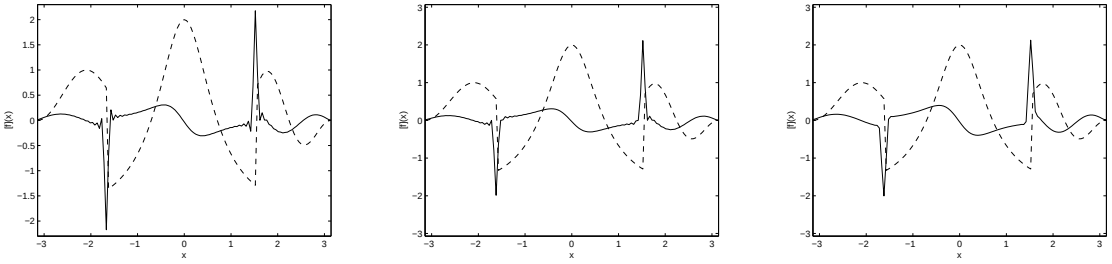

(a) **(b)** **(c)**

Figure 4: The concentration method, (4.19) with $N = 64$, applied to Example 4.1 using the trigonometric factor (4.20) with $\alpha = \pi$: (a) The original results, (b) the Lanczos factor (4.28) with $n = 1$, and (c) the matching concentration factor (4.38). In all three figures the underlying function is dashed and the jump function approximation is solid.

Another concentration factor introduced in [9] is the zero-crossing concentration factor:

$$\tau_Z\left(\frac{|k|}{N}\right) = -k\frac{\left(\tau(\frac{|k|}{N})\right)^2}{\sum_{l=1}^{N}\left(\tau(\frac{|l|}{N})\right)^2}, \tag{4.39}$$

where τ is any of the filtered or unfiltered admissible concentration factors defined earlier. The zero crossing concentration factor is derived by determining the regions corresponding to the point of the zero crossing of the second derivative approximation where the approximation of the first derivative has maximum amplitude. This version of the concentration method attempts to locate the zero crossing signature profile that can be created by the derivative projection of the concentration method (4.19). The analysis is similar to that of the matching waveform concentration method, and can be found in [9]. In this case, the concentration factors are not admissible in the traditional sense, since the concentration method using the zero crossing concentration factor converges to

$$[f](x) - \frac{1}{2}[f](x \pm 2\rho) + \mathcal{O}(\frac{\log N}{N}),$$

where ρ is the distance of the first maximum away from the jump discontinuity.

As noted in [9], there are some advantages in using the zero-crossing concentration method. Most notably, the support of the jump function approximation is in some sense reduced, so that the minmod algorithm is better able to pinpoint jump discontinuities when it is used. Figure 5 demonstrates this effect. Notice that any remaining oscillations from the previous application of minmod (see Figure 3) have been eliminated.

The jump discontinuities of the piecewise smooth function found by the edge detection method determine the regions of smoothness. We can now re-exapnd the solution in each region of smoothness using the spectral reprojection method. Section 6 demonstrates the effectiveness of filtering, edge detection, and spectral reprojection through numerical example.

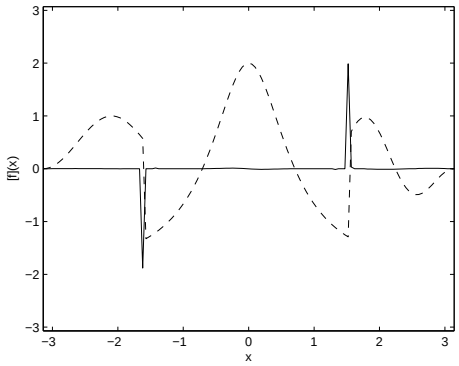

Figure 5: The minmod limiter, (4.26), applied to Example 4.1 using the concentration factor (4.20) with Lanczos filtering (4.28) and in conjunction with the matching waveform (4.38) and the zero crossing waveform (4.39) methods. The underlying function is dashed and the jump function approximation is solid.

5 Linear Equations with Discontinuous Solutions

The filtering and reprojection techniques have proven very useful when solving time dependent partial differential equations using spectral methods. However, despite compelling numerical evidence [17, 21, 39], there is no general theory that guarantees that reprojection will recover high order accuracy in numerical simulations. The question is, if spectral reprojection is used on the time-evolved solution, can the Gibbs phenomenon be eliminated and high order accuracy be restored? More specifically, does the spectal method solution of the partial differential equation retain high order information even after being convected forward in time?

This section provides a partial answer to these questions for Fourier spectral methods solutions of linear hyperbolic equations with discontinuous initial conditions. Although Fourier spectral methods (used for spatial discretization) yield only first accurate order solutions, this numerical solution retains its underlying high order information even after being convected forward in time. In turn, an exponentially accurate solution can be recovered by post-processing.[4]

To see that this is indeed the case, consider the hyperbolic problem

$$U_t = \mathcal{L}U$$

(where $\mathcal{L}$ is a semi-bounded operator) with some discontinuous initial condition

$$U(x,0) = U_0(x).$$

The Galerkin approximation is

$$\left(\frac{\partial u}{\partial t} - \mathcal{L}u, \phi_k\right)_{L^2[-\pi,\pi]} = 0$$

where ϕ is a (possibly multi-dimensional) trigonometric polynomial in x (where x may represent a vector of multiple dimensions). When $U_0(x)$ is a continuous we have the usual error estimate

$$\|u - U\|_{L^2[-\pi,\pi]} \leq cN^{-s}\|U_0\|_{H_p^s[\pi,\pi]}.$$

[4]Here we only consider Fourier spectral methods. Spectral methods using Chebyshev and Legendre polynomials for scalar nonlinear partial differential equations have been shown to be stable and to converge to the correct entropy solution, [32, 36, 40, 41, 35, 42, 43], and there is compelling numerical evidence that indeed spectral accuracy can be recovered by post-processing, [17, 21, 37, 39].

However, when $U_0(x)$ is discontinuous this error estimate is no longer valid, but we have the corresponding result in the weak sense:

Theorem 5.1 *[34] For every smooth function $\psi(x)$,*

$$|(u-U,\psi)|_{L^2[-\pi,\pi]} \leq cN^{-s}\|\psi\|_{H^s_p[-\pi,\pi]}.$$

Proof. Given a smooth function $\psi(x,t)$, we can always find a function $V(x,t)$ which is the solution of

$$\frac{\partial V}{\partial t} = -\mathcal{L}^* V \quad \text{with} \quad V(x,0) = V_0(x),$$

such that at time $t=\tau$, the two are equal $\psi(x,\tau) = V(x,\tau)$. This is always possible because we can solve the hyperbolic equation backwards and forwards, and so can pick initial conditions which give us the solution we want at time τ. Let $v(x,t)$ be the Galerkin approximation

$$\left(\frac{\partial v}{\partial t} + \mathcal{L}^* v, \phi_k\right)_{L^2[-\pi,\pi]} = 0,$$

where $\phi_k(x,t)$ is a trigonometric polynomial in x, and $v(x,0) = \mathcal{P}_N V_0$. The solutions U and V satisfy Green's identity

$$(U(\tau), V(\tau))_{L^2[-\pi,\pi]} = (U_0, V_0)_{L^2[-\pi,\pi]} \ ,$$

as can be seen from

$$\begin{aligned}
\frac{\partial}{\partial t}(U,V)_{L^2[0,2\pi]} &= (U_t, V)_{L^2[-\pi,\pi]} + (U, V_t)_{L^2[-\pi,\pi]} = (\mathcal{L}U, V)_{L^2[-\pi,\pi]} + (U, -\mathcal{L}^* V)_{L^2[-\pi,\pi]} \\
&= (\mathcal{L}U, V)_{L^2[-\pi,\pi]} - (U, \mathcal{L}^* V)_{L^2[-\pi,\pi]} = 0.
\end{aligned}$$

Similarly, by observing that both u and v are trigonometric polynomials in x, we have

$$\left(\frac{\partial u}{\partial t}, v\right)_{L^2[-\pi,\pi]} = (\mathcal{L}u, v)_{L^2[-\pi,\pi]} \quad \text{and} \quad \left(\frac{\partial v}{\partial t}, u\right)_{L^2[-\pi,\pi]} = -(\mathcal{L}^* v, u)_{L^2[-\pi,\pi]}.$$

Therefore u and v also satisfy Green's identity

$$(u(\tau), v(\tau))_{L^2[-\pi,\pi]} = (u_0, v_0)_{L^2[-\pi,\pi]}.$$

Recall that the terms $(U_0 - u_0, v_0)_{L^2[-\pi,\pi]}$ and $(u_0, V_0 - v_0)_{L^2[-\pi,\pi]}$ are zero because $(U_0 - u_0)$ and $(V_0 - v_0)$ are orthogonal to the space of trigonometric polynomials in which u_0 and v_0 live. By using Green's identity and adding and subtracting these zero terms, we obtain

$$\begin{aligned}
(U(\tau) - u(\tau), V(\tau)) &= (U(\tau), V(\tau)) - (u(\tau), V(\tau)) \\
&= (U_0, V_0) - (u(\tau), V(\tau) - v(\tau)) - (u_0, v_0) \\
&= (U_0, V_0) - (u_0, v_0) - (U_0 - u_0, v_0) + (u_0, V_0 - v_0) \\
&- (u(\tau), V(\tau) - v(\tau)) \\
&= (U_0, V_0) - (U_0, v_0) + (u_0, V_0 - v_0) - (u(\tau), V(\tau) - v(\tau)) \\
&= (U_0 + u_0, V_0 - v_0) - (u(\tau), V(\tau) - v(\tau)).
\end{aligned}$$

Since $\mathcal{L}$ is semi-bounded, the Galerkin approximation is stable, and spectral accuracy follows:

$$(U(\tau) - u(\tau), V(\tau)) \leq k_1 N^{-s}\|V_0\|_{H^s_p[-\pi,\pi]} + k_2 N^{-s}\|V(\cdot,\tau)\|_{H^s_p[-\pi,\pi]} \leq cN^{-s}\|V_0\|_{H^s_p[-\pi,\pi]}.$$

This theorem shows us that a discontinuous profile can be convected forward in time with a spectral method, and that furthermore, the numerical solution at the final time contains the necessary information to extract a high order approximation to the exact solution.

The next question is whether this fact is still true for solutions of nonlinear equations. Although it has been shown that spectral methods for scalar nonlinear equations with discontinuous solutions are stable with appropriate filtering, [32, 34], there is no theory which guarantees that high order information can be extracted from the solution by spectral reprojection. However, numerical evidence indicates that highly accurate solutions may be recovered from spectral method approximations of conservation laws in one dimension, [21, 39], as well as for shallow water equations on a sphere, [17]. To do so, we first determine the regions of smoothness of the final time solution by the edge detection method. We can now re-expand the solution in any interval of smoothness using a Gibbs complementary basis.

6 Fourier Spectral Approximation of Burgers Equation

Equipped with the results from the previous sections, we are now ready to implement a fully automated Fourier spectral method code that yields high accuracy and strongly resolves the shock discontinuities. We will consider the periodic inviscid Burgers equation:

$$\frac{\partial}{\partial t}u(x,t) + \frac{\partial}{\partial x}(\frac{u^2(x,t)}{2}) = 0, \tag{6.1}$$

where $(x,t) \in [-\pi,\pi] \times [0,\infty)$, with the initial condition $u(x,0) = \sin x$, and the prescribed periodic boundary conditions, $u(-\pi,t) = u(\pi,t)$.

In the Fourier spectral method we seek a solution of the form

$$u_N(x,t) = \sum_{k=-N}^{N} a_k(t)e^{ikx}$$

such that the equation

$$\frac{\partial}{\partial t}u_N(x,t) + \frac{\partial}{\partial x}(\frac{u_N^2(x,t)}{2}) = 0,$$

is satisfied at the gridpoints $x_j = \frac{2\pi j}{N}, \quad j \in [0,\ldots,N-1]$. This results in a system of ordinary differential equations for $a_k(t)$. This system of ODEs is evolved forward in time, based on the initial conditions, with the classical fourth order Runge-Kutta scheme. We use a time step $\Delta t = \frac{\sqrt{2}}{N\pi}$. An exponential filter is used at each time step to stabilize the scheme. The solution at time $T = 1.5$ is displayed in Figure 6. This solution is stable, but demonstrates the effects of the Gibbs phenomenon, as we see in the errors. Edge detection and Gegenbauer reconstruction are then used to produce a oscillation-free high order numerical solution, seen in Figure 7. In the post-processed solution, the time-stepping errors dominate. We emphasize that only the first step, the Fourier spectral method, is time-implemented. Subsequent steps, including the edge detection and post-processing using spectral reprojection, are only performed once, at the final time $T = 1.5$. Therefore very little extra work is required to obtain high-order accuracy.

This numerical experiment demonstrates how Fourier spectral methods use filtering to obtain a stable solution which retains high order information, so that edge detection post-processing can be applied to recover a high order solution for the discontinuous solution of the partial differential equation.

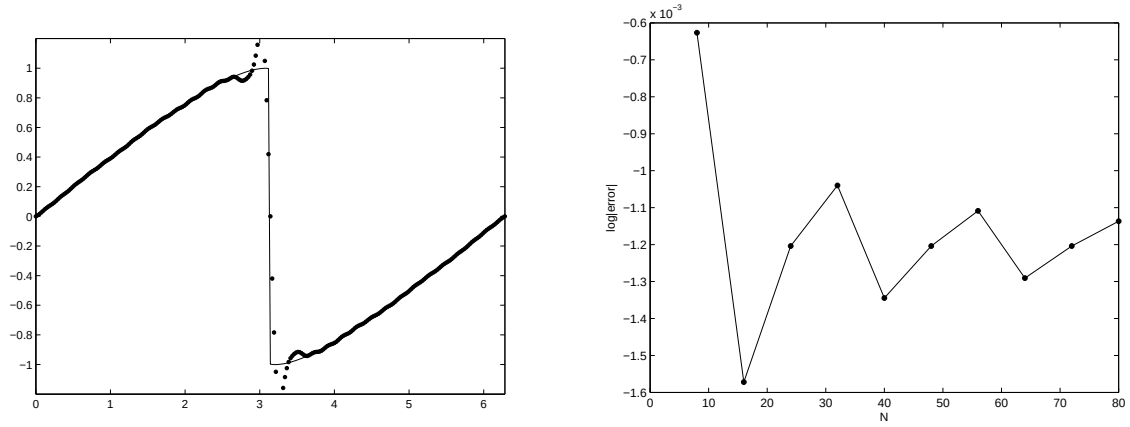

Figure 6: (a) The numerical solution of (6.1) at time $T = 1.5$ for $N = 40$ using a spectral viscosity filter. (b) The errors in logarithmic scale for the time evolved solution.

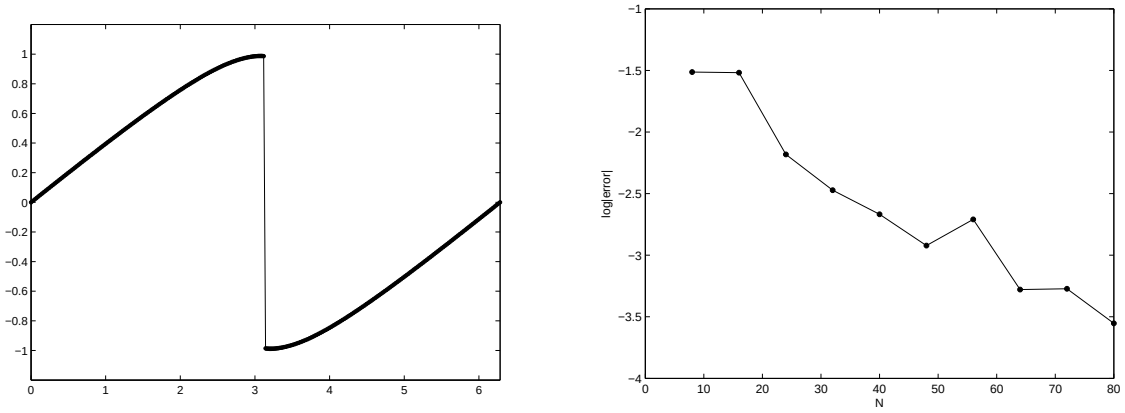

Figure 7: (a) The Gegenbauer reconstruction of the numerical solution to (6.1) at time $T = 1.5$ for $N = 40$. (b) The errors in logarithmic scale for the Gegenbauer reconstruction method.

References

[1] S. Abarbanel, D. Gottlieb and E. Tadmor, *Spectral methods for discontinuous problems*, in "Numerical Methods for Fluid Dynamics II," ed. by N.W. Morton and M.J. Baines, Oxford University Press, (1986), pp.128-153.

[2] R. Archibald and A. Gelb, *A Method to Reduce the Gibbs Ringing Artifact in MRI Scans While Keeping Tissue Boundary Integrity*, IEEE Transactions on Medical Imaging, **21** (4), (2002).

[3] N.S. Banerjee and J. Geer, *Exponentially accurate approximations to piecewise smooth periodic functions*, ICASE Report No. 95-17, NASA Langley Research Center, 1995.

[4] N. Bary, *Treatise of Trigonometric Series*, The Macmillan Company, New York, 1964.

[5] H. Bateman, Higher Transcendental Functions Volume II, McGraw-Hill Book Company, INC., 1953.

[6] R. Bauer, *Band filters for determining shock locations*, Ph.D. thesis, Applied mathematics, Brown University, 1995.

[7] J.P. Boyd, *Trouble with Gegenbauer Reconstruction for Defeating Gibbs' Phenomenon: Runge phenomenon in the diagonal limit of Gegenbauer Polynomial Approximations*, Journal of Computational Physics, **204** (2005) pp. 253-264.

[8] M. Carpenter, D. Gottlieb and C.W. Shu, *On the Conservation and Convergence to Weak Solutions of Global Schemes*, Journal of Scientific Computing **18**, (2003) pp. 111-132.

[9] D. Cates and A. Gelb, *Detection of Edges in Spectral Data III - Improvements in the Presence of Noise*, preprint.

[10] W. S. Don, *Numerical Study of Pseudospectral Methods in Shock Wave Applications*, Journal of Computational Physics, **110**, (1994) pp. 103-111.

[11] W. S. Don, C. Quillen, *Numerical simulation of Reactive Flow, Part I : Resolution*, Journal of Computational Physics **122**, (1995) pp. 244-265.

[12] W. S. Don & D. Gottlieb, *High Order Methods for Complicated Flows Interacting with Shock Waves*, AIAA 97-0538.

[13] W. S. Don & D. Gottlieb, *Spectral Simulations of Supersonic Reactive Flows*, SIAM, Journal on Numerical Analysis, **35**, (1998) pp. 2370-2384.

[14] W. S. Don, D. Gottlieb & J. H. Jung, *A multi-domain spectral method for supersonic reactive flows*, Journal of Computational Physics, **192** (2003) pp. 325 - 354.

[15] T. A. Driscoll and B. Fornberg, *A Padé-Based Algorithm for Overcoming the Gibbs Phenomenon*, Numerical Algorithms, **26** (2001) pp. 77-92.

[16] A. Gelb, *Parameter Optimization and Reduction of Round Off Error for the Gegenbauer Reconstruction Method*, Journal of Scientific Computing, **20:3** (2004) pp. 433-459.

[17] A. Gelb and J. P. Gleeson, *Spectral viscosity for shallow water equations in spherical geometry*, Monthly Weather Review, **129** (2001), pp. 2346–2360.

[18] A. Gelb and E. Tadmor, *Detection of edges in spectral data*, Applied Computational Harmonic Analysis, **7** (1999) pp. 101-135 .

[19] A. Gelb and E. Tadmor, *Detection of edges in spectral data II. Nonlinear Enhancement*, SIAM Journal on Numerical Analysis, **38:4**, (2000) pp. 1389-1408.

[20] A. Gelb and E. Tadmor, *Adaptive Edge Detectors for Piecewise Smooth Data Based on the Minmod Limiter*, Journal of Scientific Computing, to appear.

[21] A. Gelb and E. Tadmor, *Enhanced Spectral Viscosity Approximation for Conservation Laws*, Applied Numerical Mathematics, **33** (2000) pp. 1-21.

[22] A. Gelb, and Z. Jackiewicz, *Determining Analyticity for Parameter Optimization of the Gegenbauer Reconstruction Method*, SIAM Journal on Scientific Computing, **27:3** (2006) pp. 1014-1032.

[23] A. Gelb and J. Tanner, *Robust Reprojection Methods for the Resolution of the Gibbs Phenomenon*, ACHA, **20:1** (2006) pp. 3-25.

[24] D. Gottlieb and E. Tadmor, *Recovering Pointwise Values of Discontinuous Data within Spectral Accuracy*, Progress in Scientific Computing, Vol. 6 (E. M. Murman and S. S. Abarbanel, eds.), Birkhauser, Boston (1985) pp. 357-375.

[25] D. Gottlieb, C. W. Shu, A. Solomonoff, H. Vandeven, *On the Gibbs phenomenon I: recovering exponential accuracy from the Fourier partial sum of a non-periodic analytic function*, Journal of Computational and Applied Mathematics **43**, (1992) pp. 81-98.

[26] D. Gottlieb, C. W. Shu, *Resolution properties of the Fourier method for discontinuous waves*, Computer Methods in Applied Mechanics and Engineering **116**, (1994) pp. 27-37.

[27] D. Gottlieb, C. W. Shu, *On the Gibbs phenomenon IV: recovering exponential accuracy in a sub-interval from a Gegenbauer partial sum of a piecewise analytic function*, Mathematics of Computation **64**, (1995) pp. 1081-1095.

[28] D. Gottlieb, C. W. Shu, *On the Gibbs phenomenon V: recovering exponential accuracy from collocation point values of a piecewise analytic function*, Numerische Mathematik **71**, (1995) pp. 511-526.

[29] D. Gottlieb, C. W. Shu, *On the Gibbs phenomenon III: recovering exponential accuracy in a sub-interval from a spectral partial sum of a piecewise in a sub-interval from a spectral partial sum of a piecewise analytic function*, SIAM Journal on Numerical Analysis **33**, (1996) pp. 280-290.

[30] D. Gottlieb, C. W. Shu, *The Gibbs phenomenon and its resolution*, SIAM Review, 39, (1997) pp.644-668.

[31] D. Gottlieb and C.W. Shu *General theory for the resolution of the Gibbs phenomenon*, Accademia Nazionale Dei Lincey, ATTI Dei Convegni Lincey **147**, (1998) pp. 39-48.

[32] D. Gottlieb and J. Hesthaven, *Spectral methods for hyperbolic problems*, Journal of Computational Applied Mathematics **128**, (2001) 83-131.

[33] A. Harten, *High resolution schemes for hyperbolic conservation laws*, Journal of Computational Physics **49** (1983), 357-393.

[34] J. S. Hesthaven, S. Gottlieb, and D. Gottlieb, *Spectral Methods for Time Dependent Problems*. Cambridge University Press (2007).

[35] Y. Maday, S. Ould Kaber, E. Tadmor, *Legendre Pseudospectral Viscosity Method for Nonlinear Conservation Laws*, SIAM Journal on Numerical Analysis **30**, (1993) pp. 321-342.

[36] H. Ma, *Chebyshev-Legendre Super Spectral Viscosity Method for Nonlinear Conservation Laws*, SIAM Journal on Numerical Analysis **35**, (1998) pp. 893-908.

[37] M.S. Min, T.W. Lee, P.F. Fischer, S.K. Gray, *Fourier Spectral Simulations and Gegenbauer Reconstructions for Electromagnetic Waves in the Presence of a Metal Nanoparticle*, Journal of Computational Physics, **213:2**, (2006) pp. 730-747.

[38] B. Shizgal and J.-H. Jung, *Towards the Resolution of the Gibbs Phenomena*, Journal of Computational Applied Mathematics, **161**, (2003) pp. 41-65.

[39] C.-W. Shu and P. Wong, *A note on the accuracy of spectral method applied to nonlinear conservation laws*, Journal of Scientific Computing, **10** (1995), pp. 357-369.

[40] E. Tadmor, *Convergence of spectral methods for nonlinear conservation laws*, SIAM Journal on Numerical Analysis **26**, (1989) pp. 30-44.

[41] E. Tadmor, *Shock capturing by the spectral viscosity method*, Proceedings of ICOSAHOM 89, Elsevier Science Publishers B. V., North Holland, IMACS (1989)

[42] E. Tadmor, *Convergence of spectral methods for nonlinear conservation laws.* SIAM Journal on Numerical Analysis **26** (1989) pp. 30-44.

[43] E. Tadmor, *Approximate solutions of nonlinear conservation laws*, in "Advanced Numerical Approximation of Nonlinear Hyperbolic Equations" Lecture notes in Mathematics **1697**, Springer Verlag (1998).

[44] H. Vandeven, *Family of spectral filters for discontinuous problems*, SIAM Journal on Scientific Computing **48**, (1991) pp. 159-192.

[45] A. Zygmund, *Trigonometric Series*, Cambridge University Press, 1959.